DOI: 10.1002/ejic.200600336

Redox Behavior of a Manganese Porphyrin Complexed with Per-*O*-methylated β-Cyclodextrin in Aqueous Solution

Koji Kano,*[a] Hiroaki Kitagishi,[a] Yumiko Sone,[a] Nami Nakazawa,[a] and Masahito Kodera[a]

Keywords: Macrocyclic ligands / Manganese / Redox chemistry / Cyclodextrins / Electrochemistry

[5,10,15,20-Tetrakis(*p*-sulfonatophenyl)porphyrinato]-manganese(III) in its diaqua form $[(H_2O)_2Mn^{III}(tpps)]$ forms a complex with heptakis(2,3,6-tri-*O*-methyl)-β-cyclodextrin (TMe-β-CD) to afford a stable 2:1 host–guest inclusion complex whose binding constants, K_1 and K_2, in phosphate buffer at pH 7.0 and 25 °C are 8.1×10^5 and 2.8×10^4 M^{-1}, respectively. $[(H_2O)_2Mn^{III}(tpps)]$ dissociates into the monohydroxo complex $[(H_2O)(OH^-)Mn^{III}(tpps)]$ above pH 11 (pK_a = 11.9) when incorporated into the TMe-β-CD cavities. The pK_a value of $[(H_2O)_2Mn^{III}(tpps)]$ in the absence of TMe-β-CD is 12.4, which suggests that the monohydroxo form without a net charge on the central porphyrin is stabilized by complexation with TMe-β-CD. In an aqueous alkaline solution of TMe-β-CD, $[(H_2O)(OH^-)Mn^{III}(tpps)]$ is autoreduced to $[(H_2O)Mn^{II}(tpps)]$ by an electron transfer from bound OH^- to Mn^{III}. TMe-β-CD stabilizes the low-valent $[(H_2O)Mn^{II}(tpps)]$. For example, the rate of autoxidation of $[(H_2O)Mn^{II}(tpps)]$ in the presence of TMe-β-CD at pH 7.0 was reduced by a factor of 2.8×10^4 as compared with the rate without TMe-β-CD. The redox potentials ($E_{1/2}$) of [Mn(tpps)] were measured by spectroelectrochemical methods. The $E_{1/2}$ values in phosphate buffer at pH 7.0 in the absence and the presence of TMe-β-CD are –211 and –108 mV (vs. NHE), respectively. TMe-β-CD causes a positive shift of $E_{1/2}$, which indicates the stabilization of low-valent $[(H_2O)Mn^{II}(tpps)]$ by TMe-β-CD against autoxidation. These electrochemical data, as well as the thermodynamic ones, give the K_1K_2 values for complexation of $[(H_2O)Mn^{II}(tpps)]$ with TMe-β-CD to be 1.2×10^{12} M^{-2}, while that for $[(H_2O)_2Mn^{III}(tpps)]$ is 2.3×10^{10} M^{-2}.

Introduction

Although manganese porphyrins (MnPor) are not known to be prosthetic groups of metalloproteins, they have widely been utilized as functional models of metalloproteins such as the manganese-stabilizing protein in photosynthesis II,[1] cytochrome P450,[2] superoxide dismutases,[3] catalases,[4] and peroxidases.[5] MnPors have many advantages when it comes to mimicking the functions of metalloproteins. For example, they have poor ability to form μ-oxo dimers[6] and to bind inorganic anions[7] and have a high ability to resist degradation of their ligands and to take various high-valent metal states.[8] The modeling of cytochrome P450 function using MnPor is a typical example. The formation of an Fe^{IV}=O cation radical, the so-called "compound I", has not been proved in artificial systems, although such a high-valent iron-oxo complex has been assumed as a dominant intermediate in oxygenation catalyzed by cytochrome P450.[9] Meanwhile, a high-valent Mn^{V}=O porphyrin complex has been verified spectroscopically when a porphyrin ligand has positively charged pyridinium substituents at the *meso* positions of the porphyrin.[10] The Mn^{V}=O complex is a reactive intermediate in the epoxidation of alkenes by *m*-CPBA. Mn^{V}=O corrole with a Mn out-of-plane orientation is more stable than the corresponding porphyrin complex with a Mn in-plane orientation.[8d,11] MnPors have mainly been utilized as substitutes of heme and/or hemin.

Since the prominent function of a metalloprotein is apparently dominated by its prosthetic group, the main interest of chemists tends to be focused on the chemical behavior of this group. In general, however, a protein surrounding the prosthetic group plays an essential role in its biological activity. Therefore, construction of a model system involving functions of both the protein and prosthetic group is a very important subject in biomimetic chemistry.[12] There are various kinds of hemoproteins in nature. In spite of a common prosthetic group (heme), each hemoprotein shows different functions. A typical example of the inherent characteristics is the oxidation-reduction potentials of hemoproteins (see Supporting Information).[13] Although myoglobin (Mb), hemoglobin (Hb), and peroxidases have a common

[a] Department of Molecular Science and Technology, Faculty of Engineering, Doshisha University,
Kyotanabe, Kyoto 610-0321, Japan
Fax: +81-774-65-6845
E-mail: kkano@mail.doshisha.ac.jp

Supporting information for this article is available on the WWW under http://www.eurjic.org or from the author.

core structure composed of an iron center and an imidazole moiety as an axial monoligand, their redox potentials differ. The redox potentials of Mb (+50 mV vs. NHE) and Hb (+170 mV) are positive, meaning low reactivity in autoxidation of heme to hemin, with these proteins having particular affinity for dioxygen binding. On the other hand, cytochrome c peroxidase has a redox potential of –194 mV. The redox potential of cytochrome P450cam with cysteine as an axial ligand is –300 mV. Hemoproteins with negative redox potentials tend to form high-valent iron complexes as active intermediates in their enzymatic reactions. The protein surrounding an iron center regulates the redox potential and hence the functions of the hemoprotein.

In the present study, we focused on the effects of incorporation of [5,10,15,20-tetrakis(*p*-sulfonatophenyl)porphyrinato]manganese [Mn(tpps)] by heptakis(2,3,6-tri-*O*-methyl)-β-cyclodextrin (TMe-β-CD) on the redox behavior of [Mn(tpps)] in aqueous solution. We,[14] as well as Tonellato et al.,[15] have reported the extremely strong ability of TMe-β-CD to include water-soluble porphyrins to afford *trans*-type 2:1 host–guest complexes. Previously, we interpreted the novel ability of TMe-β-CD to include the water-soluble porphyrins in terms of induced-fit-type inclusion by TMe-β-CD, whose cavity is transformable because of the absence of intramolecular hydrogen bonding.[14d] Recently, we also found metMb-mimetic functions of a 2:1 complex of TMe-β-CD and [Fe^{III}(tpps)], which shows selective binding of inorganic anions in aqueous solution.[16] In advance of our study, Lawrence and co-workers reported their pioneering work on a hemoprotein mimic composed of a cationic ferric porphyrin and heptakis(2,6-di-*O*-methyl)-β-cyclodextrin (2,6-DMe-β-CD).[17] These results led us to prepare a Mb model that works in aqueous solution.[18] Since the 1970s, many Mb models have been proposed.[19] Typically, these models have bulky substituents at the *meso* positions of tetraphenylporphyrin to prevent μ-oxo dimer formation. Although those model compounds whose ferrous center is coordinated by a base such as imidazole or pyridine bind dioxygen in absolute organic solvents, no dioxygen adducts are formed if the system contains a trace amount of water. Recently, we succeeded in preparing a Mb model (hemoCD) in aqueous solution that is composed of an *O*-methylated β-cyclodextrin dimer containing a pyridine linker and [Fe^{II}(tpps)].[18] HemoCD binds dioxygen in aqueous solution ($P_{1/2}^{O_2}$ = 16.9 Torr and $t_{1/2}$ = 30 h in pH 7.0 phosphate buffer at 25 °C). In this model system, tight encapsulation of [Fe^{II}(tpps)] by two *O*-methylated β-cyclodextrin moieties is essential to stabilize [Fe^{II}(tpps)] and to bind dioxygen. As an extension of this work, we decided to study the redox behavior of a manganese porphyrin complexed with TMe-β-CD. In the present study, we tried to obtain information about the effects of TMe-β-CD on the stabilization of the low-valent manganese complex [$(H_2O)Mn^{II}$(tpps)]. In order to prepare a good functional model of Mb and/or Hb, the system should be designed to stabilize Fe^{II}Por, which is labile in a homogeneous aerobic solution, by using an artificial protein such as cyclodextrin. Control of the redox potential of a metalloporphyrin by an artificial protein is essential to develop a new artificial and functional metalloprotein. The present study might contribute to these subjects.

Results and Discussion

Complexation of [Mn^{II}(tpps)], [Mn^{III}(tpps)], and [Mn^{IV}(tpps)] with TMe-β-CD

At first, complexation of [Mn^{III}(tpps)] with TMe-β-CD was studied by means of UV/Vis spectroscopy and isothermal titration calorimetry (ITC). Figure 1 shows the UV/Vis spectral changes of [$(H_2O)_2Mn^{III}$(tpps)] in 0.05 M phosphate buffer at pH 7.0 upon addition of TMe-β-CD. The Soret band at 466 nm is shifted to shorter wavelength and increases in intensity with increasing concentration of TMe-β-CD. Three titration curves obtained by monitoring the absorbances at three different wavelengths were fitted simultaneously by a set of binding constants (K_1 and K_2) using a nonlinear least-squares method (Figure 1, b).[14b]

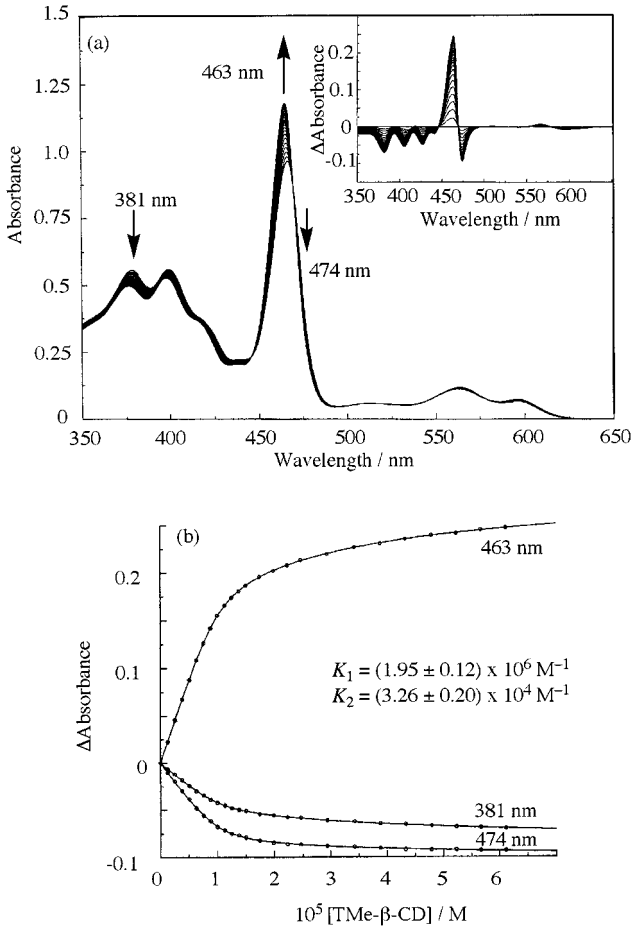

Figure 1. UV/Vis spectral changes of [$(H_2O)_2Mn^{III}$(tpps)] (1.0×10^{-5} M) in 0.05 M phosphate buffer at pH 7.0 upon addition of TMe-β-CD at 25 °C (a) and the plots of the changes in absorbances of [$(H_2O)_2Mn^{III}$(tpps)] vs. [TMe-β-CD] (b). The solid lines are the best fit of the data to an equation for the simultaneous 1:1 and 1:2 complexation.

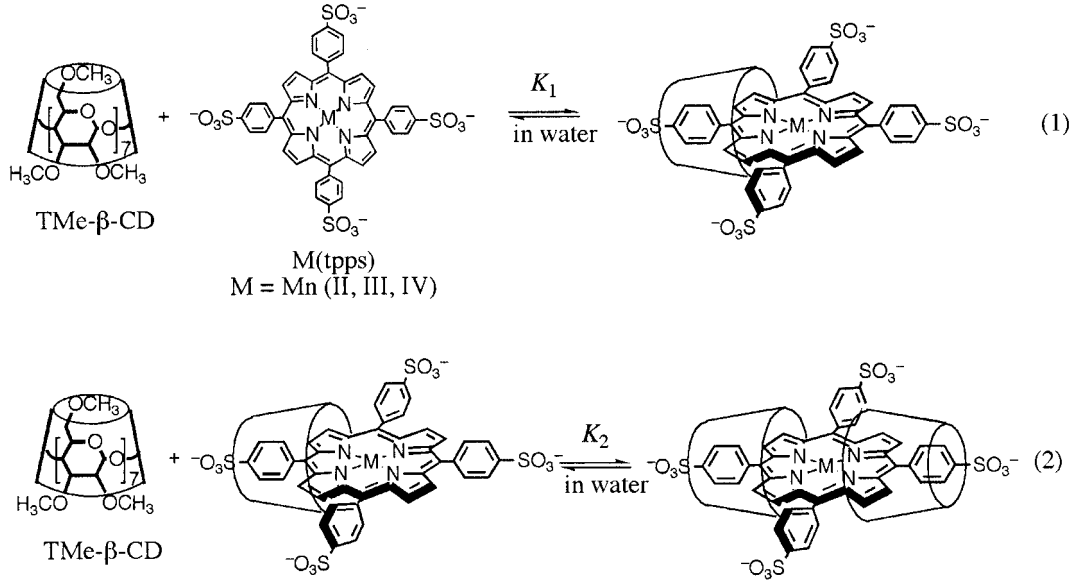

Figure 2. Complexation of MnPor with TMe-β-CD in aqueous solution.

Table 1. Binding constants and thermodynamic parameters for complexation of M(tpps) (M = Mn^{II}, Mn^{III}, Mn^{IV} and Fe^{III}) in aqueous solution at 25 °C.

M(tpps)	Method	$10^{-6}\cdot K_1$ [M^{-1}]	$10^{-4}\cdot K_2$ [M^{-1}]	ΔH^0_1 [kJ mol^{-1}]	ΔS^0_1 [mol^{-1} K^{-1}]	ΔH^0_2 [kJ mol^{-1}]	ΔS^0_2 [J mol^{-1} K^{-1}]	Ref.
Mn^{III}	UV[a]	2.0 ± 0.1	3.3 ± 0.2	–	–	–	–	this work
Mn^{III}	ITC[a]	0.81 ± 0.13	2.8 ± 0.2	–49 ± 1	–50 ± 3	–22 ± 1	11 ± 2	this work
Fe^{III}	ITC[b]	1.3 ± 0.1	6.3 ± 0.4	–49 ± 1	–47 ± 1	–12 ± 1	53 ± 1	[16]
Mn^{II}	UV, ITC[c]	too large	too large	–	–	–	–	this work
Mn^{IV}	ITC[d]	0.34 ± 0.11	7.5 ± 1.3	–25 ± 1	21 ± 6	–6 ± 1	73 ± 4	this work

[a] In 0.05 M phosphate buffer at pH 7.0. [b] In 0.1 M succinic acid buffer at pH 4.0. [c] In 0.05 M phosphate buffer at pH 7.0. The measurement was carried out in the presence of excess $Na_2S_2O_4$. [d] In 1.0 M aqueous NaOH solution. [(OH^-)Mn^{IV}(tpps)] was prepared by oxidation of [$(H_2O)_2Mn^{III}$(tpps)] with three equivalents of $K_3[Fe(CN)_6]$.

The titration curves were well-fitted by a theoretical equation for 2:1 host–guest complexation. The K_1 and K_2 values (Figure 2) were determined to be $(2.0 \pm 0.1) \times 10^6$ and $(3.3 \pm 0.2) \times 10^4$ M^{-1}, respectively (Table 1).

We decided to check the accuracy of the binding constants by a different method (ITC). ITC simultaneously provides the thermodynamic parameters for complexation of [$(H_2O)_2Mn^{III}$(tpps)] with TMe-β-CD. The isothermal calorimetric titration curve obtained by the addition of TMe-β-CD to the [$(H_2O)_2Mn^{III}$(tpps)] solution at pH 7.0 is shown in Figure 3. The titration curve was analyzed by an equation for 2:1 host–guest complex formation; the results are summarized in Table 1. The K_1 and K_2 values from ITC are somewhat smaller than those from UV/Vis spectroscopy; the reasons for this are not clear. However, both methods clearly indicate that K_1 is larger than K_2. Since tpps is a dianionic ligand, a positive charge remains at the center of [$(H_2O)_2Mn^{III}$(tpps)]. Capping of such a polar metal center by two hydrophobic cyclodextrin cavities seems to be inadequate compared with the 1:1 complexation where half of the metalloporphyrin is exposed to the bulk aqueous phase. This might be the reason why K_1 is larger than K_2. Such an assumption is supported by the thermodynamic parameters for complexation. Both enthalpy ($\Delta H_1{}^0$) and entropy changes ($\Delta S_1{}^0$) for the 1:1 complexation are negative and large, thereby suggesting the contribution of a van der Waals interaction to the 1:1 complex formation as a main binding force. The negative and large value of $\Delta S_1{}^0$ is ascribed to the restriction of free rotation of the sulfonatophenyl groups at the 10- and 20-positions of the porphyrin due to inclusion of a sulfonatophenyl group at the 5-position. The complexation of the 1:1 complex with TMe-β-CD to form a 2:1 complex is accompanied by a positive $\Delta S_2{}^0$. From this observation we assume that dehydration which is needed for further complexation supports the formation of the 2:1 complex.

As mentioned below, [Mn^{III}(tpps)] exists in a diaqua form [$(H_2O)_2Mn^{III}$(tpps)] in aqueous solution at pH 7.0. Under the same conditions, the ferric porphyrin [Fe^{III}(tpps)] forms a μ-oxo dimer in the absence of TMe-β-CD. Since the apparent pK_a value for the equilibrium between [$(H_2O)_2Fe^{III}$(tpps)] and the μ-oxo dimer is 6.4,[20] the K_1 and K_2 values for [$(H_2O)_2Fe^{III}$(tpps)] in aqueous solution below pH 5 seem to be meaningful to compare with those for [$(H_2O)_2Mn^{III}$(tpps)]. The binding constants and the thermodynamic parameters for [$(H_2O)_2Fe^{III}$(tpps)] at pH 4.0 are shown in Table 1.[16] A similar behavior has been observed in the complexation of [$(H_2O)_2Fe^{III}$(tpps)] with

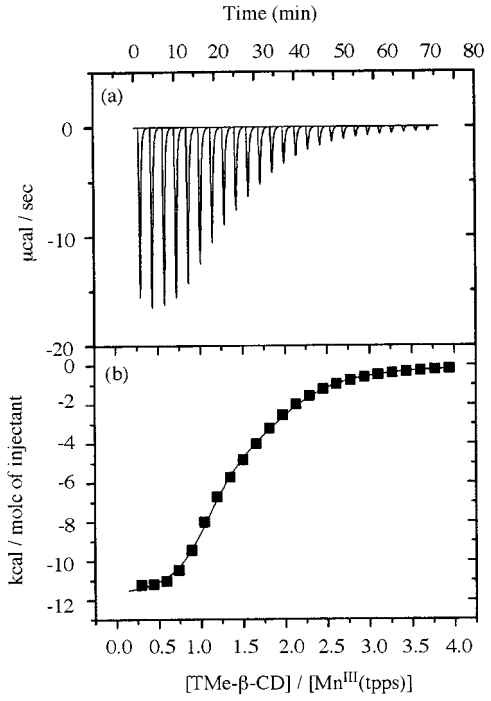

Figure 3. Calorimetric titration of $[(H_2O)_2Mn^{III}(tpps)]$ (2.28×10^{-4}) with 25 aliquots (10 μL each) of TMe-β-CD (4.79×10^{-3} M) in 0.05 M phosphate buffer at pH 7.0 and 25 °C. The solid line represents the best fit of the experimental data to the 1:2 Sequential Binding Sites Model in the ORIGIN software.

TMe-β-CD, although the ΔS^0 value for $[(H_2O)_2Fe^{III}(tpps)]$ is much larger than that for $[(H_2O)_2Mn^{III}(tpps)]$.

$[(H_2O)_2Mn^{III}(tpps)]$ is easily reduced to $[(H_2O)Mn^{II}(tpps)]$ by sodium dithionite ($Na_2S_2O_4$). The UV/Vis spectral changes of $[(H_2O)Mn^{II}(tpps)]$ in pH 7.0 phosphate buffer containing an excess amount of $Na_2S_2O_4$ were monitored as a function of the concentration of TMe-β-CD (see Supporting Information). The spectral change was clearly saturated upon addition of two equivalents of TMe-β-CD, thus indicating the formation of an extremely stable 2:1 host–guest complex. Binding constants and thermodynamic parameters for $[(H_2O)Mn^{II}(tpps)]$ could not be determined by either UV/Vis spectroscopy or ITC because of the too-large K values, although the K_1K_2 value was estimated (vide infra). Since the net charge at the center of $[(H_2O)Mn^{II}(tpps)]$ is zero, the encapsulation of $[(H_2O)Mn^{II}(tpps)]$ by two TMe-β-CD molecules seems to proceed satisfactorily from the viewpoint of polarity matching between the host and the guest.

$[Mn^{III}(tpps)]$ was oxidized to $[Mn^{IV}(tpps)]$ in 1.0 M aqueous NaOH solution upon addition of $K_3[Fe(CN)_6]$.[21] A strongly basic solution is needed to stabilize the high-valent Mn^{IV} state by coordination of OH^- to Mn^{IV}. In the presence of an excess amount of TMe-β-CD, the second-order rate constant (k_{ox}) for oxidation of $[(H_2O)(OH^-)Mn^{III}(tpps)]$ to $[(OH^-)_nMn^{IV}(tpps)]$ (n = 1 or 2) was determined to be 50.1 $M^{-1}s^{-1}$ at 25 °C (Figure 4). Harriman et al. have determined the k_{ox} value for the same oxidation in the absence of TMe-β-CD to be 1.08×10^5 $M^{-1}s^{-1}$.[21] It is clear that encapsulation of $[(H_2O)(OH^-)Mn^{III}(tpps)]$ by two TMe-β-CD molecules markedly depresses the oxidation by the polar ferricyanide ion. In other words, the TMe-β-CD molecules provide a very hydrophobic environment around the center of $[(H_2O)(OH^-)Mn^{III}(tpps)]$ that isolates it from the aqueous bulk phase.

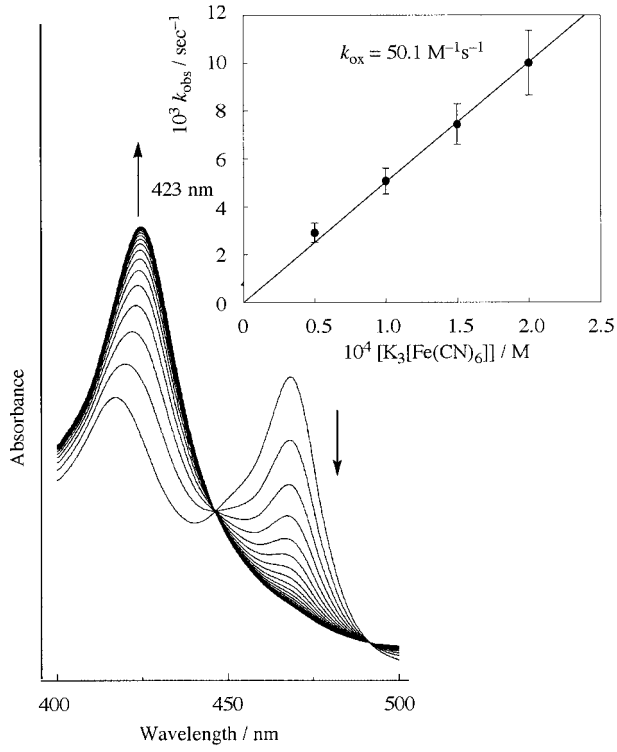

Figure 4. UV/Vis spectral changes of $(H_2O)(OH^-)Mn^{III}(tpps)$ (1.0×10^{-5} M) to $[(OH^-)Mn^{IV}(tpps)]$ in 1.0 M aqueous NaOH solution containing TMe-β-CD (2.0×10^{-4} M) upon addition of $K_3[Fe(CN)_6]$ (1.0×10^{-4} M) at 25 °C and the dependence of the pseudo first-order rate constant (k_{obs}) for the oxidation of $(H_2O)(OH^-)Mn^{III}(tpps)$ to $[(OH^-)Mn^{IV}(tpps)]$ on the concentration of $K_3[Fe(CN)_6]$ to determine the second-order rate constant (k_{ox}).

The K_1 and K_2 values for complexation of $[(OH^-)_nMn^{IV}(tpps)]$ with TMe-β-CD were determined in 1.0 M aqueous NaOH solution by ITC (see Supporting Information). The results are shown in Table 1. To the best of our knowledge, the axial ligation of $[Mn^{IV}(tpps)]$ in aqueous NaOH solution has not been clarified. If $[Mn^{IV}(tpps)]$ exists as $[(OH^-)Mn^{IV}(tpps)]$, the net charge at the center of the porphyrin is +1, the same as that of $[(H_2O)_2Mn^{III}(tpps)]$. The K_1 and K_2 values for $[(OH^-)_nMn^{IV}(tpps)]$ in aqueous NaOH solution are not much different from those of $[(H_2O)_2Mn^{III}(tpps)]$ at pH 7.0. However, the thermodynamic parameters for $[(OH^-)Mn^{IV}(tpps)]$ differ markedly from those for $[(H_2O)_2Mn^{III}(tpps)]$. The entropy change for the 1:1 complexation of $[(OH^-)_nMn^{IV}(tpps)]$ is positive while that of $[(H_2O)_2Mn^{III}(tpps)]$ is negative and large. The entropy change for the second complexation of $[(OH^-)_nMn^{IV}(tpps)]$ is also larger than that of $[(H_2O)_2Mn^{III}(tpps)]$. It is assumed that the high-valent Mn^{IV} porphyrin gathers a larger amount of water molecules to its metal center than

the Mn^{III} porphyrin. It is interesting that complexation of high-valent $[(OH^-)_nMn^{IV}(tpps)]$ is entropically favorable due to extended dehydration while it is enthalpically unfavorable due to weak hydrophobic effect. Complexation promoted by extended dehydration is commonly observed in cyclodextrin chemistry.[22] The difference between the thermodynamic parameters of $[(OH^-)_nMn^{IV}(tpps)]$ and $[(H_2O)_2Mn^{III}(tpps)]$ might be ascribed to the difference in the net charges of the manganese porphyrins. In other words, there is a possibility of $[(OH^-)_2Mn^{IV}(tpps)]$ rather than $[(OH^-)Mn^{IV}(tpps)]$. The axial ligation of $[Mn^{IV}(tpps)]$ in aqueous alkaline solution could not be clarified from the present study.

pH Titration

$[Mn^{III}(tpps)]$ exists as a diaqua form in aqueous solution at neutral pH.[6a] An increase in pH up to 11 did not cause any UV/Vis spectral change for $[(H_2O)_2Mn^{III}(tpps)]$ (λ_{max} = 465 nm) in aqueous solution containing TMe-β-CD. However, the absorption spectrum changes markedly above pH 11 (Figure 5) and the pH-titration curve gave a pK_a of 11.9. Since the isosbestic points are observed clearly, there should only be an equilibrium in the pH range between 2.5 and 13.5. The most reasonable process is the acid dissociation of $[(H_2O)_2Mn^{III}(tpps)]$ to $[(H_2O)(OH^-)Mn^{III}(tpps)]$. In the absence of TMe-β-CD, the pK_a value was determined to be 12.4, somewhat lower than that of the $[(H_2O)_2Mn^{III}$-(tpps)]/TMe-β-CD complex. Such a result means that $[(H_2O)(OH^-)Mn^{III}(tpps)]$ is stabilized by complexation with TMe-β-CD. Harriman et al. have reported two pK_a values (8.6 and 11.6) for $[Mn^{III}(tpps)]$ in aqueous solution without cyclodextrin.[6a] However, we could not observe the equilibrium corresponding to pK_a 8.6. It should be noted that a weak absorption band was observed at 433 nm in the higher pH region. The absorption maximum of this band is in good agreement with that of $[(H_2O)Mn^{II}(tpps)]$. This band did not affect the isosbestic points, which suggests only an equilibrium in this system. Such a contradiction might be ascribed to the formation of only a small amount of $[(H_2O)Mn^{II}(tpps)]$.

Autoreduction of $[Mn^{III}(tpps)]$ in Aqueous Alkaline Solution

Figure 6 shows the absorption spectral changes of $[(H_2O)(OH^-)Mn^{III}(tpps)]$ in 1.0 M aqueous NaOH solution containing TMe-β-CD at 50 °C under a nitrogen atmosphere. The absorbance at 463 nm due to $[(H_2O)(OH^-)$-$Mn^{III}(tpps)]$ gradually decreases and a band with a peak at 434 nm, which is ascribed to $[(H_2O)Mn^{II}(tpps)]$, appears. $[(H_2O)(OH^-)Mn^{III}(tpps)]$ is autoreduced to $[(H_2O)Mn^{II}$-(tpps)] in aqueous alkaline solution under anaerobic conditions. Since such an autoreduction occurs only in aqueous alkaline solution, the OH^- ion must participate in this reduction. Clear isosbestic points indicate the quantitative nature of this reaction. Arasasingham and Bruice have reported that [5,10,15,20-tetrakis(2,4,6-trimethylphenyl)porphyrinato]manganese(III) $[Mn^{III}(tmp)]$ is reduced to $[Mn^{II}$-(tmp)] in CH_3CN containing methanolic tetrabutylammonium hydroxide.[23] Jeon et al. have also studied the autoreduction of [5,10,15,20-tetrakis(2,6-dichlorophenyl)porphyrinato]manganese(III) $[Mn^{III}(tcp)]$ in CH_3CN containing aqueous tetraethyl hydroxide.[24] Both groups reported the formation of five-coordinate $[(L)Mn^{II}Por]$ complexess (L: solvent; λ_{max} = 436–437 nm) via $[(L)(OH^-)Mn^{III}Por]$ and/or $[(L)(CH_3O^-)Mn^{III}Por]$. As a next step, ligand exchange of $[(L)Mn^{II}Por]$ to $[(OH^-)Mn^{II}Por]$ (λ_{max} = 444–445 nm) proceeds. The former group assumed further conversion of

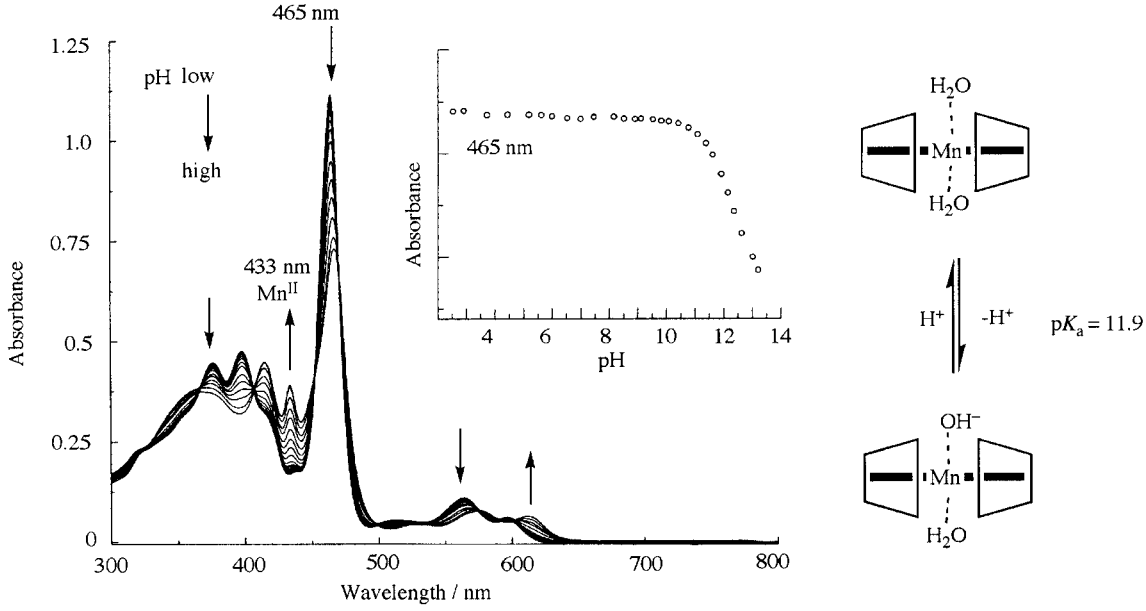

Figure 5. UV/Vis spectral changes of $Mn^{III}(tpps)$ (1.0×10^{-5} M) in aqueous TMe-β-CD (1.0×10^{-3} M) solution in the presence of 0.1 M $NaClO_4$ as a function of pH.

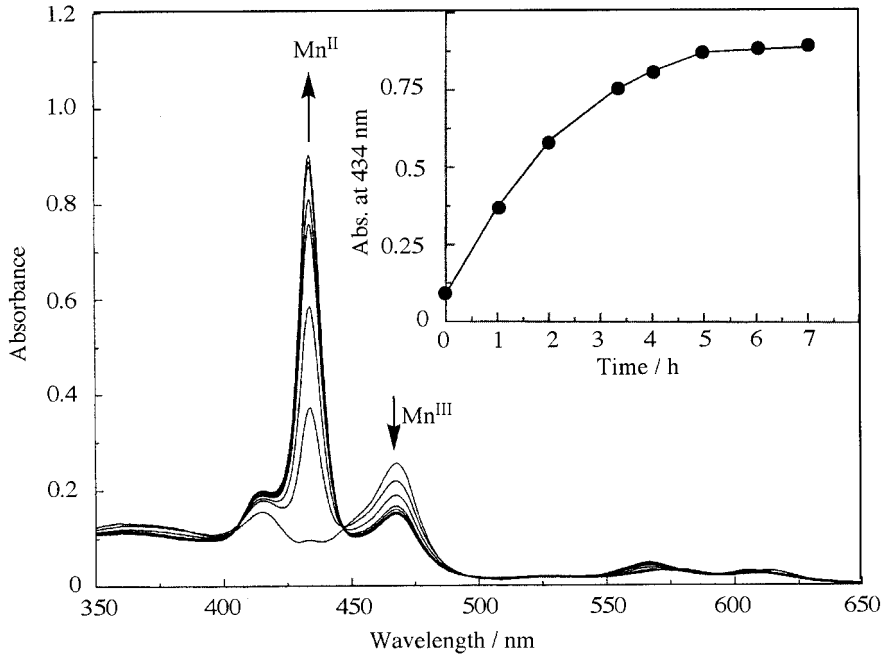

Figure 6. Progressive UV/Vis spectral changes of $[(H_2O)(OH^-)Mn^{III}(tpps)]$ (5.0×10^{-6} M) to $[(H_2O)Mn^{II}(tpps)]$ in 1.0 M aqueous NaOH solution containing TMe-β-CD (1.0×10^{-4} M) at 50 °C under N_2. Inset: time course in absorbance at 434 nm due to $[(H_2O)Mn^{II}(tpps)]$.

$[(OH^-)Mn^{II}(tmp)]$ to a mixture of $[(OH^-)_2Mn^{III}(tmp)]$, $[(OH^-)(CH_3O^-)Mn^{III}(tmp)]$, and $[(CH_3O^-)_2Mn^{III}(tmp)]$ with absorption maxima at 412 and 448 nm, although the mechanism was not clarified.[23] The present system is simpler than the systems in CH_3CN. Only autoreduction of $[(H_2O)(OH^-)Mn^{III}(tpps)]$ to $[(H_2O)Mn^{II}(tpps)]$ occurs in 1.0 M aqueous NaOH solution containing TMe-β-CD at 50 °C. We measured the pH-dependent absorption spectral change of $[(H_2O)Mn^{II}(tpps)]$ complexed with TMe-β-CD and could not find any spectral change in the pH range between 3.0 and 13.5, therefore no equilibrium exists between $[(H_2O)Mn^{II}(tpps)]$ and $[(OH^-)Mn^{II}(tpps)]$ under the present conditions. In the absence of TMe-β-CD, no autoreduction occurred in 1.0 M aqueous NaOH solution. Although we did not study the mechanism of the autoreduction in detail, one-electron transfer from bound OH^- to the Mn^{III} center might occur, as demonstrated by Sawyer and co-workers, who found that the oxidation potentials of OH^- and a phenoxide ion in CH_3CN shift to less positive potentials upon coordination to $[Mn^{III}Por]$.[25] As a preliminary experiment, we measured the ESI mass spectrum (positive mode) of the $CHCl_3$ extract of a reaction mixture obtained by heating a mixture of TMe-β-CD (1×10^{-3} M) in 1.0 M aqueous NaOH solution containing $[(H_2O)(OH^-)Mn^{III}(tpps)]$ (5×10^{-4} M) at 70 °C for 16 h. The molecular ion peaks were observed at *m/z* 1438.6, 1452.6, 1468.6, and 1550.6, which correspond to $[(TMe\text{-}β\text{-}CD - OCH_3 + OH + Na)^+$; calcd. 1438.2], $[(TMe\text{-}β\text{-}CD + Na)^+$; calcd. 1452.5], $[(TMe\text{-}β\text{-}CD + K)^+$; calcd. 1468.6], and $[(TMe\text{-}β\text{-}CD + CHCl_3 + H)^+$; calcd. 1550.9], respectively (see Supporting Information). These results strongly suggest that generated $^{\cdot}OH$ radical reacts with TMe-β-CD leading to replacement of an OCH_3 group of TMe-β-CD with an OH group.

Stabilization of Low-Valent $[(H_2O)Mn^{II}(tpps)]$ by TMe-β-CD

As shown in Figure 5, the autoreduction occurs even under aerobic conditions if TMe-β-CD is present in the system. We therefore studied the effects of TMe-β-CD on stabilization of $[(H_2O)Mn^{II}(tpps)]$. Oxidation of $[(H_2O)Mn^{II}(tpps)]$ was carried out by bubbling oxygen through asolution of $[(H_2O)Mn^{II}(tpps)]$, which was prepared by the reaction of $[(H_2O)_2Mn^{III}(tpps)]$ with $Na_2S_2O_4$ in phosphate buffer at pH 7.0. In the absence of TMe-β-CD, $[(H_2O)Mn^{II}(tpps)]$ (λ_{max} = 432 nm) was oxidized at once to $[(H_2O)_2Mn^{III}(tpps)]$ (λ_{max} = 466 nm) immediately after $S_2O_4^{2-}$ disappeared upon oxidation with O_2 (Supporting Information). In the presence of TMe-β-CD, however, the autoxidation of $[(H_2O)Mn^{II}(tpps)]$ to $[(H_2O)_2Mn^{III}(tpps)]$ occurs gradually (Figure 7), thus indicating that low-valent $[(H_2O)Mn^{II}(tpps)]$ is stabilized against autoxidation by complexation with TMe-β-CD.

The pseudo-first-order rate constants for autoxidation of $[(H_2O)Mn^{II}(tpps)]$ (1.7×10^{-6} M) in 0.05 M phosphate buffer containing TMe-β-CD (3.4×10^{-5} M) at pH 7.0 and 25 °C were determined as a function of partial dioxygen pressure (see Supporting Information). The second-order rate constant (k) for the autoxidation was determined to be 5.4 $M^{-1}s^{-1}$. In the absence of TMe-β-CD, the second-order rate constant has been reported to be 1.5×10^5 $M^{-1}s^{-1}$.[26] Encapsulation of $[(H_2O)Mn^{II}(tpps)]$ by two TMe-β-CD molecules drastically depresses the autoxidation. Such a phenomenon is quite similar to the effect of globin on the stabilization of a ferrous porphyrin (heme) against autoxidation.

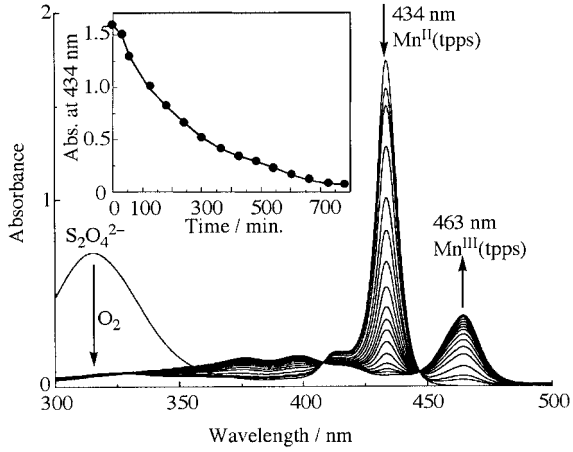

Figure 7. UV/Vis spectral changes of $[(H_2O)Mn^{II}(tpps)]$ (5.0×10^{-6} M) in 0.05 M phosphate buffer at pH 7.0 and 25 °C in the presence of TMe-β-CD (1.0×10^{-4} M) after bubbling O_2 gas through the solution. $[(H_2O)Mn^{II}(tpps)]$ was prepared by the reduction of $[(H_2O)_2Mn^{III}(tpps)]$ with an excess amount of $Na_2S_2O_4$. Inset: The time course in absorbance at 434 nm due to $[(H_2O)Mn^{II}(tpps)]$ after O_2 bubbling.

There are two plausible mechanisms for autoxidation of $[(H_2O)Mn^{II}Por]$ (Figure 8). Mechanism 1 is an outer-sphere electron-transfer mechanism where the electron transfer occurs intermolecularly. Mechanism 2 is similar to the mechanism proposed for autoxidation of oxy-myoglobin[27] and its model oxy-hemoCD.[18b] Dioxygen complexes of Mn^{II} porphyrin complexes are known to be formed in organic solvents at low temperature.[28] To the best of our knowledge, the dioxygen adduct of Mn^{II}Por has not been detected at ambient temperature, meaning that the dioxygen adduct of Mn^{II} porphyrin is very unstable. In Mechanism 2, the rate-determining step of the autoxidation must be the ligand-exchange step of $[(H_2O)Mn^{II}Por]$ to $[(O_2)Mn^{II}Por]$ because the autoxidation obeys second-order kinetics. In our previous work, we determined the rate constant for dioxygen association to the iron(II) center of hemoCD to be 4.7×10^7 $M^{-1}s^{-1}$.[18b] The penetration of dioxygen into the cleft formed by the *O*-methylated β-cyclodextrin dimer is extremely fast. The cleft of hemoCD should be much less labile than the present case, where the cleft is formed intermolecularly by two TMe-β-CD molecules. The less labile nature of hemoCD is ascribed to the lower mobility of the cyclodextrin moieties linked to each other by a covalent bond and to ligation of the pyridine moiety involved in the linker to the Fe^{II} center. On the basis of these considerations, mechanism 2 can be excluded. In other words, $[(H_2O)Mn^{II}(tpps)]$ seems to be oxidized by an outer-sphere electron-transfer mechanism (mechanism 1). Since the penetration of dioxygen into the cleft formed by two TMe-β-CD molecules is expected to be a fast process, the marked stabilization of $[(H_2O)Mn^{II}(tpps)]$ by the TMe-β-CD molecules is not ascribed to the encapsulation effect due to tight blocking of the Mn^{II} center. One possibility that explains the stabilization of low-valent $[(H_2O)Mn^{II}(tpps)]$ is alteration of the redox potential of [Mn(tpps)] upon inclusion into the TMe-β-CD cavities. We therefore measured the redox potentials of [Mn(tpps)] in the absence and presence of TMe-β-CD.

Redox Potential of $[(H_2O)_2Mn^{III}(tpps)]$

At first, cyclic voltammetry (CV) was applied to determine the Mn^{III}-Mn^{II} redox potential of $[(H_2O)_2Mn^{III}$-(tpps)]. In the absence of TMe-β-CD, CV provided a redox potential, $E_{1/2}$, of –410 mV (vs. Ag/AgCl) in 0.05 M phosphate buffer at pH 7.0 containing 0.1 M Na_2SO_4 as supporting electrolyte (see Supporting Information). In the presence of TMe-β-CD, however, no redox peak appeared because the metal center of $[(H_2O)_2Mn^{III}(tpps)]$ is blocked by two TMe-β-CD molecules. It has been shown that an electrode reaction is strictly inhibited by inclusion of a sample in cyclodextrin.[29] Ribo et al. measured the cyclic voltammograms of Mn^{III}(tpps) complexed with cyclodextrins such as α-cyclodextrin and 2-hydroxypropyl-β-cyclodextrin.[6b] They assumed the electrode reactions of the Mn(tpps)-cyclodextrin complexes adsorbed on the electrode. We were unable to observe any redox peak when TMe-β-CD, a stronger host for water-soluble porphyrins, was added to the system, therefore we decided to use a spectroelectrochemical method, which is the established method to determine the redox potential of metalloenzymes as well as metal complexes,[30] to study the electrochemistry of the Mn(tpps)/TMe-β-CD complex.

The Nernst equation [Equation (1)] applied to an electrode reaction is

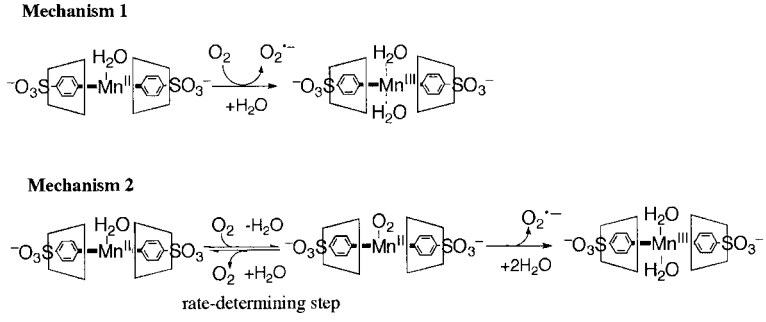

Figure 8. Plausible mechanisms for autoxidation of $[(H_2O)Mn^{II}(tpps)]$ complexed with TMe-β-CD.

$$E = E_{1/2} + [(RT)/(nF)]\ln(a_{Ox}/a_{Red}) \quad (1)$$

where E and $E_{1/2}$ are the actual potential and the standard redox potential, respectively, and a_{Ox} and a_{Red} are the chemical activities of the chemical species on the oxidized and reduced electrodes, respectively. R, T, and F are the gas constant, the absolute temperature, and the Faraday constant, respectively. Equation (1) can be transformed into Equation (2), which is the equation for a one-electron redox reaction at 25 °C applicable to a spectroelectrochemical measurement.

$$E = E_{1/2} + 0.05914\log[(A_{Red} - A)/(A - A_{Ox})] \quad (2)$$

where A is the experimentally observed absorbance of a sample at E and a certain wavelength and A_{Red} and A_{Ox} are the absorbances of the reduced and oxidized species, respectively, at the same wavelength. In order to accelerate the electrode reaction, 9,10-anthraquinone-2-sulfonate ($E_{1/2}$ = –442 mV vs. Ag/AgCl)[31] was used as an electron mediator. The UV/Vis spectral changes of [Mn(tpps)] in phosphate buffer containing 0.1 M Na_2SO_4 as a function of applied potential (E = –200 to –475 mV vs. Ag/AgCl) are shown in Figure 9. The spectral changes as a function of E indicate the existence of only equilibrium between $[(H_2O)_2Mn^{III}(tpps)]$ and $(H_2O)Mn^{II}(tpps)$. From the Nernst plot, the $E_{1/2}$ value for the Mn^{III}-Mn^{II} redox of the Mn(tpps)/TMe-β-CD complex was determined to be –320 ± 3 mV at pH 7.0 and 25 °C. A similar spectroelectrochemical titration provided an $E_{1/2}$ value of –423 ± 8 mV for [Mn(tpps)] in phosphate buffer (pH 7.0) without TMe-β-CD (see Supporting Information). Interestingly, complexation of [Mn(tpps)] with TMe-β-CD causes a positive shift of $E_{1/2}$ by about 100 mV, which suggests stabilization of low-valent $[(H_2O)Mn^{II}(tpps)]$ against autoxidation by TMe-β-CD. The free-energy change (ΔG^0) during a redox reaction can be evaluated from Equation (3).

$$\Delta G^0 = -nFE_{1/2} \quad (3)$$

The free-energy changes for the equilibria shown in Figure 10 were calculated from the $E_{1/2}$ values and the binding constants for complexation of $[(H_2O)_2Mn^{III}(tpps)]$ and TMe-β-CD. The ΔG^0 value for the redox reaction of [Mn(tpps)] in the presence of TMe-β-CD is 10 kJ mol^{-1}, while that for the system in the absence of TMe-β-CD is 20 kJ mol^{-1}. From the thermodynamic and electrochemical data, the K_1K_2 value for the complexation of $[(H_2O)Mn^{II}$-(tpps)] with TMe-β-CD to form a 2:1 host–guest complex can be calculated to be 1.2×10^{12} M^{-2}. In the case of $[(H_2O)_2Mn^{III}(tpps)]$, the K_1K_2 value is 2.3×10^{10} M^{-2}. It is clear that a positive net charge remaining on the center of $[(H_2O)_2Mn^{III}(tpps)]$ greatly destabilizes the 2:1 host–guest complex.

Although we also measured the Mn^{III}-Mn^{IV} redox potentials in aqueous alkaline solutions with and without TMe-β-CD, we could not obtain reliable data to compare the redox potential of the Mn(tpps)/TMe-β-CD complex with that of free [Mn(tpps)] (see Supporting Information).

Conclusions

The present study leads to the following conclusions:
(1) The 1:2 inclusion complex of $[(H_2O)Mn^{II}(tpps)]$ and TMe-β-CD is much more stable than that of $[(H_2O)_2Mn^{III}$-(tpps)] and TMe-β-CD. Destabilization of $[(H_2O)_2Mn^{III}$-(tpps)]/TMe-β-CD is ascribed to a positive net charge remaining on the center of the metalloporphyrin;
(2) $[(H_2O)(OH^-)Mn^{III}(tpps)]$ in aqueous alkaline solution containing TMe-β-CD gradually changes to $[(H_2O)Mn^{II}$-

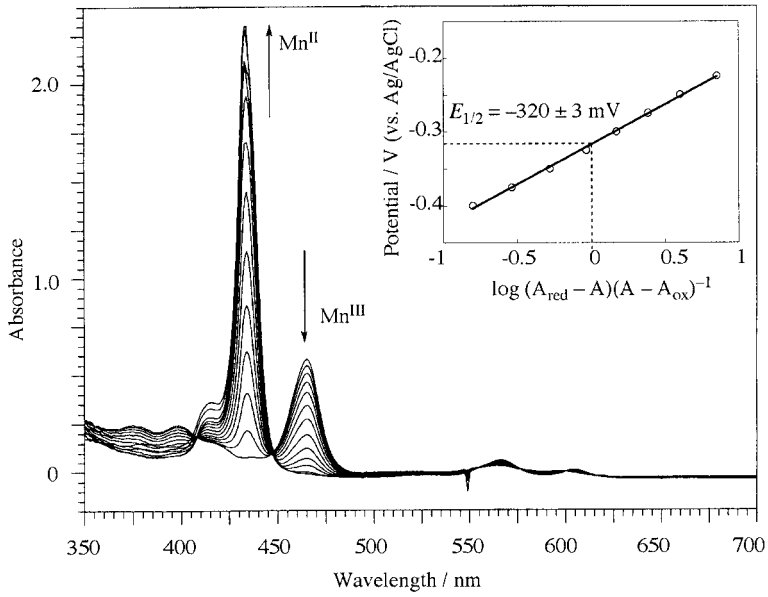

Figure 9. UV/Vis spectral changes of [Mn(tpps)] (5.0×10^{-5} M) in 0.05 M phosphate buffer containing 5.0×10^{-4} M TMe-β-CD and 0.1 M Na_2SO_4 at various applied potentials (E = –200 to –475 mV vs. Ag/AgCl) during the spectroelectrochemical titration at pH 7.0 and 25 °C. Inset: the Nernst plot obtained from the spectral changes at 463 nm.

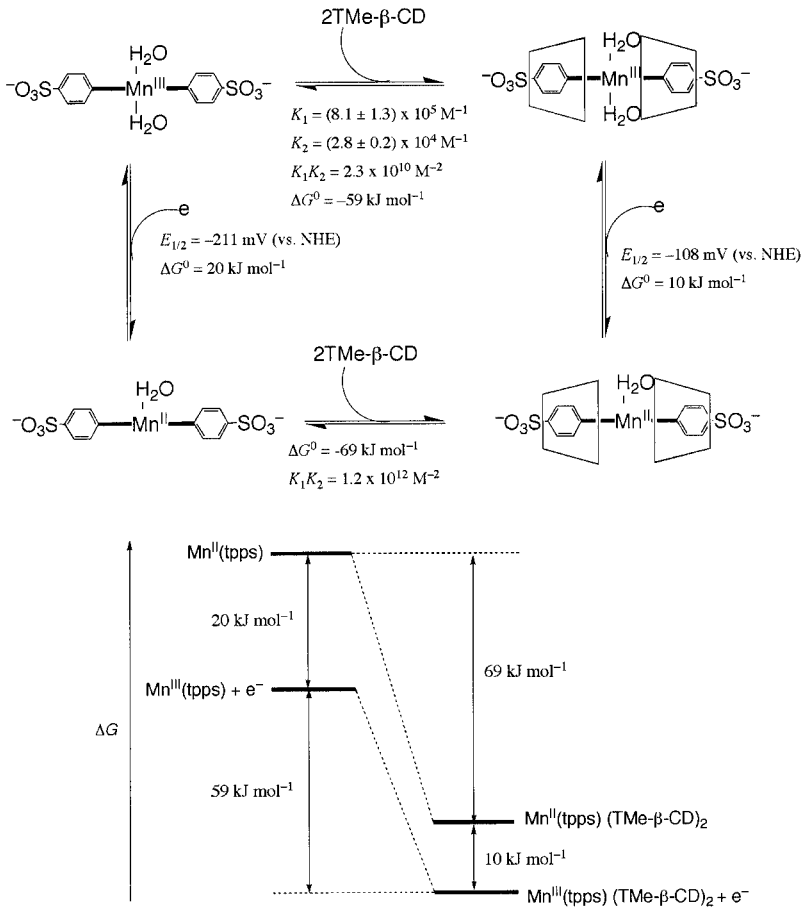

Figure 10. Free-energy changes for the equilibria of the Mn(tpps)/TMe-β-CD system in aqueous solution at pH 7.0 and 25 °C.

(tpps)] through a one-electron transfer from bound OH^- to Mn^{III}. Formation of low-valent [$(H_2O)Mn^{II}$(tpps)] is detectable even under aerobic conditions because of marked stabilization due to incorporation of [$(H_2O)Mn^{II}$(tpps)] into the TMe-β-CD cavities;

(3) The redox potentials of [Mn(tpps)] in pH 7.0 phosphate buffer are –211 and –108 mV (vs. NHE) in the absence and the presence of TMe-β-CD, respectively. [$(H_2O)Mn^{II}$(tpps)] is stabilized against autoxidation by complexation with TMe-β-CD, which mimics the function of proteins in biological systems.

Experimental Section

Materials: [5,10,15,20-Tetrakis(*p*-sulfonatophenyl)porphyrinato]-manganese(III) chloride in an acidic form (Frontier Scientific), TMe-β-CD (Nacalai), and anthraquinone-2-sulfonate sodium salt (Nacalai) were purchased and used as received. On the basis of the extinction coefficient of [$(H_2O)_2Mn^{III}$(tpps)] ($\varepsilon_{466} = 9.5 \times 10^4$), the purchased manganese porphyrin was determined to be the hexahydrate. Water was purified with a Millipore Simpak 1 apparatus. Pure O_2 (99.999%) and pure N_2 (99.999%) gases were purchased from Sumitomo Seika Chemicals.

Measurements: UV/Vis spectra were recorded with a Shimadzu UV-2450 spectrophotometer with a thermostatted cell holder. The pH values were measured with a Horiba pH meter M-12. Determination of the binding constants for the complexation of [Mn(tpps)] with TMe-β-CD was performed from the UV/Vis spectral titrations according to a published method.[14b,16] Microcalorimetric measurements were carried out using a Microcal Isothermal Titration Calorimeter VP-ITC. The titration curve obtained was analyzed using the Sequential Binding Sites Model for 2:1 host–guest complexation in the ORIGIN software program.[32]

Mixed O_2 gases with various partial pressures in N_2 were prepared with a KOFLOC GM-4B gas-mixing apparatus.

Cyclic voltammetry was carried out with a BAS CV-50W electrochemical analyzer. A gold working electrode, a platinum counter electrode, and a Ag/AgCl (3 M NaCl) reference electrode were utilized in a single-component cell. The working electrode was polished with 0.05-μm alumina and washed with pure water prior to use. The measurements were carried out under a N_2 atmosphere.

The spectroelectrochemical measurements were carried out using an optically transparent thin-layer electrode cell (BAS, optical length: 0.5 mm). A working platinum mesh electrode ($7 \times 8 \times 0.2\ mm^3$, 80 mesh) was immersed in the cell. A platinum wire and Ag/AgCl (3 M NaCl) were used as the counter and reference electrodes, respectively. The potential was controlled by a potentiostat system (ALS1100A electrochemical analyzer, BAS). The UV/Vis spectra during electronic reduction were recorded with a Shimadzu Multispec-1500 spectrometer with a thermostatted cell holder. Anthraquinone-2-sulfonate was used to mediate electron transfer between the Mn(tpps)/TMe-β-CD complex and the working electrode. The measurements were carried out at 25 °C under

N_2. The UV/Vis spectral changes at various applied potentials were analyzed by using a Nernst equation to determine the redox potential between Mn^{II}(tpps) and Mn^{III}(tpps).[31,33]

Supporting Information (see also the footnote on the first page of this article): Redox potentials of hemoproteins (Table S1), UV/Vis spectral changes of [$(H_2O)Mn^{II}$(tpps)] as a function of [TMe-β-CD] (Figure S1), ITC for complexation of [$(OH^-)_nMn^{IV}$(tpps)] with TMe-β-CD (Figure S2), ESI mass spectrum of a reaction mixture of [$(H_2O)Mn^{II}$(tpps)] and TMe-β-CD in aqueous alkaline solution (Figure S3), UV/Vis spectra of [$(H_2O)Mn^{II}$(tpps)] and its oxidized product in phosphate buffer without TMe-β-CD (Figure S4), plot of the pseudo-first-order rate constant for autoxidation of [$(H_2O)Mn^{II}$(tpps)] in phosphate buffer with TMe-β-CD vs. [O_2] (Figure S5), CVs. of [Mn(tpps)] in phosphate buffer with and without TMe-β-CD (Figure S6), spectroelectrochemical data of [Mn(tpps)] in phosphate buffer without TMe-β-CD (Figure S7), and Mn^{III}-Mn^{IV} redox behavior of [Mn(tpps)] in aqueous alkaline solutions with and without TMe-β-CD.

Acknowledgments

This study was supported by Grants-in-Aid for Scientific Research B (nos. 14340224 and 17350074) and on Scientific Research for Priority Area (no. 16041243) from the Ministry of Education, Culture, Sports, Science and Technology, Japan.

[1] Y. Naruta, M. Sasayama, T. Sasaki, *Angew. Chem.* **1994**, *106*, 1964–1965; *Angew. Chem. Int. Ed. Engl.* **1994**, *33*, 1839–1841.
[2] a) H. Zhou, J. T. Groves, *J. Porphyrins Phthalocyanines* **2004**, *8*, 125–140; b) J. Yang, B. Gabriele, S. Belvedere, Y. Huang, R. Breslow, *J. Org. Chem.* **2002**, *67*, 5057–5067; c) R. Breslow, *Chem. Rec.* **2001**, *1*, 3–11; d) Z. Fang, R. Breslow, *Org. Lett.* **2006**, *8*, 251–254.
[3] a) V. L. Pecoraro, M. J. Baldwin, A. Gelasco, *Chem. Rev.* **1994**, *94*, 807–826; b) I. Batinic-Haberle, I. Spasojevic, P. Hambright, L. Benov, A. L. Crumbliss, I. Fridovich, *Inorg. Chem.* **1999**, *38*, 4011–4022.
[4] a) V. L. Pecoraro, M. J. Baldwin, A. Gelasco, *Chem. Rev.* **1994**, *94*, 807–826; b) N. N. Gerasimchuk, A. Gerges, T. Clifford, A. Danby, K. Bowman-James, *Inorg. Chem.* **1999**, *38*, 5633–5636.
[5] R. Weiss, V. Bulach, A. Gold, J. Terner, A. X. Trauwein, *J. Biol. Inorg. Chem.* **2001**, *6*, 831–845.
[6] a) A. Harriman, G. Porter, *J. Chem. Soc., Faraday Trans. 2* **1979**, *75*, 1532–1542; b) O. Ramirez-Gutierrez, J. Claret, J. M. Ribo, *J. Porphyrins Phthalocyanines* **2005**, *9*, 368–376; c) S.-P. Chen, D. Ejeh, D. Levermore, H. Griffith, Y. Bullen, C. M. Hosten, P. Hambright, *J. Phys. Chem. B* **1998**, *102*, 9101–9108.
[7] S. L. Kelly, K. M. Kadish, *Inorg. Chem.* **1982**, *21*, 3631–3639.
[8] a) I. Tabushi, N. Koga, *J. Am. Chem. Soc.* **1979**, *101*, 6456–6458; b) P. Bhyrappa, J. K. Young, J. S. Moore, K. S. Suslik, *J. Am. Chem. Soc.* **1996**, *118*, 5708–5711; c) Y. Shimazaki, T. Nagano, H. Takesue, B.-H. Ye, F. Tani, Y. Naruta, *Angew. Chem.* **2004**, *116*, 100–102; *Angew. Chem. Int. Ed.* **2004**, *43*, 98–100; d) S. P. de Visser, F. Ogliaro, Z. Gross, S. Shaik, *Chem. Eur. J.* **2001**, *7*, 4954–4960; e) R. Weiss, V. Bulach, A. Gold, J. Terner, A. X. Trautwein, *J. Biol. Inorg. Chem.* **2001**, *6*, 831–845.
[9] a) Y. Watanabe, *J. Biol. Inorg. Chem.* **2001**, *6*, 846–856; b) S. Shaik, S. P. de Visser, D. Kumar, *J. Biol. Inorg. Chem.* **2004**, *9*, 661–668; c) S. Jin, T. A. Bryson, J. H. Dawson, *J. Biol. Inorg. Chem.* **2004**, *9*, 644–653; d) C. Jung, V. Schünemann, F. Lendzian, *Biochem. Biophys. Res. Commun.* **2005**, *338*, 355–364; e) M. Newcomb, R. E. P. Chandrasena, *Biochem. Biophys. Res. Commun.* **2005**, *338*, 394–403.
[10] a) J. T. Groves, J. Lee, S. S. Marla, *J. Am. Chem. Soc.* **1997**, *119*, 6269–6273; b) N. Jin, J. T. Groves, *J. Am. Chem. Soc.* **1999**, *121*, 2923–2924.
[11] a) Z. Gross, G. Golubkov, L. Simkhovich, *Angew. Chem.* **2000**, *112*, 4211–4213; *Angew. Chem. Int. Ed.* **2000**, *39*, 4045–4047; b) S. P. de Visser, F. Ogliaro, Z. Gross, S. Shaik, *Chem. Eur. J.* **2001**, *7*, 4954–4960.
[12] Y. Murakami, J. Kikuchi, Y. Hisaeda, O. Hayashida, *Chem. Rev.* **1996**, *96*, 721–758.
[13] J. A. Cowan, *Inorganic Biochemistry: An Introduction*, 2nd ed., Wiley-VCH, New York, **1997**.
[14] a) K. Kano, N. Tanaka, H. Minamizono, Y. Kawakita, *Chem. Lett.* **1996**, 925–926; b) K. Kano, R. Nishiyabu, T. Asada, Y. Kuroda, *J. Am. Chem. Soc.* **2002**, *124*, 9937–9944; c) K. Kano, R. Nishiyabu, T. Yamazaki, I. Yamazaki, *J. Am. Chem. Soc.* **2003**, *125*, 10625–10634; d) K. Kano, R. Nishiyabu, R. Doi, *J. Org. Chem.* **2005**, *70*, 3667–3673.
[15] T. Carofiglio, R. Fornasier, V. Lacchini, C. Rosso, U. Tonellato, *Tetrahedron Lett.* **1996**, *37*, 8019–8022.
[16] K. Kano, H. Kitagishi, S. Tamura, A. Yamada, *J. Am. Chem. Soc.* **2004**, *126*, 15202–15210.
[17] D. L. Dick, T. V. S. Rao, D. Sukumaran, D. S. Lawrence, *J. Am. Chem. Soc.* **1992**, *114*, 2664–2669.
[18] a) K. Kano, H. Kitagishi, M. Kodera, S. Hirota, *Angew. Chem.* **2005**, *117*, 439–442; *Angew. Chem. Int. Ed.* **2005**, *44*, 435–438; b) K. Kano, H. Kitagishi, C. Dagallier, M. Kodera, T. Matsuo, T. Hayashi, Y. Hisaeda, S. Hirota, *Inorg. Chem.* **2006**, *45*, 4448–4460; c) K. Kano, H. Kitagishi, S. Tanaka, *J. Incl. Phenom. Macrocycl. Chem.*, DOI: 10.1007/S10847-006-9063-8.
[19] a) J. P. Collman, *Acc. Chem. Res.* **1977**, *10*, 265–272; b) T. G. Traylor, *Acc. Chem. Res.* **1981**, *14*, 102–109; c) M. Momenteau, C. A. Reed, *Chem. Rev.* **1994**, *94*, 659–698; d) J. P. Collman, R. Boulatov, C. J. Sunderland, L. Fu, *Chem. Rev.* **2004**, *104*, 561–588.
[20] S. Mosseri, J. C. Mialocq, B. Perly, P. Hambright, *J. Phys. Chem.* **1991**, *95*, 4659–4663.
[21] N. Carnieri, A. Harriman, G. Porter, *J. Chem. Soc., Dalton Trans.* **1982**, 931–938.
[22] a) K. Kano, T. Kitae, Y. Shimofuri, N. Tanaka, Y. Mineta, *Chem. Eur. J.* **2000**, *6*, 2705–2713; b) K. Kano, H. Hasegawa, *J. Am. Chem. Soc.* **2001**, *123*, 10616–10627.
[23] R. D. Arasasingham, T. C. Bruice, *Inorg. Chem.* **1990**, *29*, 1422–1427.
[24] S. Jeon, H. K. Lee, Y.-K. Choi, *Bull. Korean Chem. Soc.* **1996**, *17*, 929–934.
[25] a) P. K. S. Tsang, P. Cofré, D. T. Sawyer, *Inorg. Chem.* **1987**, *26*, 3604–3609; b) D. T. Sawyer, J. L. Roberts Jr, *Acc. Chem. Res.* **1988**, *21*, 469–476.
[26] I. A. Duncan, A. Harriman, G. Porter, *J. Chem. Soc., Faraday Trans. 2* **1980**, *76*, 1415–1428.
[27] K. Shikama, *Chem. Rev.* **1998**, *98*, 1357–1373.
[28] a) C. J. Weschler, B. M. Hoffman, F. Basolo, *J. Am. Chem. Soc.* **1975**, *97*, 5278–5280; b) B. M. Hoffman, T. Szymanski, T. G. Brown, F. Basolo, *J. Am. Chem. Soc.* **1978**, *100*, 7253–7259; c) R. D. Jones, D. A. Summerville, F. Basolo, *J. Am. Chem. Soc.* **1978**, *100*, 4416–4424; d) A. Weselucha-Birczynska, L. M. Proniewicz, K. Bajdor, K. Nakamoto, *J. Raman Spectrosc.* **1991**, *22*, 315–319.
[29] a) T. Matsue, D. H. Evans, T. Osa, N. Kobayashi, *J. Am. Chem. Soc.* **1985**, *107*, 3411–3417; b) A. Mirzoian, A. E. Kaifer, *Chem. Eur. J.* **1997**, *3*, 1052–1058.
[30] For example: a) K. M. Kadish, J. Shao, Z. Ou, R. Zhan, F. Burdet, J.-M. Barbe, P. Gros Claude, R. Guilard, *Inorg. Chem.* **2005**, *44*, 9023–9038; b) X. Zhao, N. Yeung, Z. Wang, Z. Guo, Y. Lu, *Biochemistry* **2005**, *44*, 1210–1214.
[31] a) L. S. Reid, V. T. Taniguchi, H. B. Gray, A. G. Mauk, *J. Am. Chem. Soc.* **1982**, *104*, 7516–7519; b) T. Matsuo, H. Dejima, S. Hirota, D. Murata, H. Sato, T. Ikegami, H. Hori, Y. Hisaeda, T. Hayashi, *J. Am. Chem. Soc.* **2004**, *126*, 16007–16017.

[32] *ITC Data Analysis in Origin - Tutorial Guide*, MicroCal, Northampton, **1998**; pp. 76–78.
[33] a) J. A. Zahn, D. M. Arciero, A. B. Hooper, A. A. Dispirito, *Eur. J. Biochem.* **1996**, *240*, 684–691; b) D. P. Hildebrand, H. Tang, Y. Luo, C. L. Hunter, M. Smith, G. D. Brayer, A. G. Mauk, *J. Am. Chem. Soc.* **1996**, *118*, 12909–12915; c) H. Sawai, N. Kawada, K. Yoshizato, H. Nakajima, S. Aono, Y. Shiro, *Biochemistry* **2003**, *42*, 5133–5142.

Received: April 14, 2006
Published Online: August 7, 2006

